Article ID: 1003 - 6326(2004)02 - 0218 - 05

Structural transformation and rheological processes in bulk metallic glass $Zr_{41}Ti_{14}Cu_{12.5}Ni_{10}Be_{22.5}$①

WANG Jing-feng(王敬丰), PU Jian(蒲 健), ZOU Hui(邹 辉),
GAN Zhang-hua(甘章华), LIU Lin(柳 林), XIAO Jian-zhong(肖建中)
(State Key Lab of Die and Mould Technology, Department of Materials Science and Engineering,
Huazhong University of Science and Technology, Wuhan 430074, China)

Abstract: The temperature dependence of strain and strain rate of the $Zr_{41}Ti_{14}Cu_{12.5}Ni_{10}Be_{22.5}$ (Vit1) bulk metallic glass (BMG) under constant heating condition was derived from the static extension method with a dynamic thermal mechanical analyzer (DMA). A few strain rate peaks, which corresponds to the glass transition and multistep crystallization in the differential scanning calorimeter (DSC) examination, were observed in the curves of the relation between strain rate and temperature. The onset of viscous flow and the end of glass transition are interrelated, the first and second strain rate peaks correspond with the first and second crystallization transition processes, respectively. The influence of stress on strain and strain rate was researched. It is found that the rheological behaviour of BMG Vit1 changes from elasticity to anelasticity, finally to the Newtonian viscous flow along with increasing temperature.

Key words: bulk metallic glass; glass transition; crystallization; rheological behavior
CLC number: TG 139 **Document code:** A

1 INTRODUCTION

Since the first success of preparing an amorphous phase in Au-Si system by rapid solidification in 1960 by Duwez et al[1], large numbers of works had been dealing with the structure transformation and properties of metallic glasses. However, the investigation on structure transformation and property in undercooled liquid state was not available because conventional metallic glasses have not distinct glass transition and a wide supercooled liquid region (SLR). Up to recent decade, a series of multicomponent metallic alloys such as La-Al-Ni[2], Pd-Ni-Cu-P[3], Zr-Al-Ni-Cu[4] and Zr-Ti-Cu-Ni-Be[5] with superior glass-forming ability and high thermal stability against crystallization were discovered. Such metallic glasses provided perfect experimental materials for investigation of structure transformation and many physical property in metallic glass.

Among these new bulk glasses forming metallic alloys, $Zr_{41}Ti_{14}Cu_{12.5}Ni_{10}Be_{22.5}$ is by far the best glass former, with a critical cooling rate of approximately 1 K/s[6]. This alloy exhibits high resistance with respect to crystallization in its wide SLR and can be cast in sizes of up to 2 cm to 4 cm in thickness. A lot of experiments[6-11] have shown that in this alloy, the primary crystallization is preceded by phase separation in the SLR. The material exhibits superplastic flow above its glass transition temperature (623 K) and strain rates of up to $1\ s^{-1}$[12]. In addition, the high yield stress[13] and the high strength to density ratio of BMG Vit1 make the material an excellent candidate for structural applications. A lot of its thermophysical properties such as heat capacity[14], diffusion[15], crystallization kinetics[16] and viscosity [7] had been well investigated.

For its deformation behavior, the previous studies mostly made use of both uniaxial compression[12, 17, 18] and three-point beam-bending[7]. However, it is seldom reported that the extension method has been applied to study the deformation of BMG Vit1. In this article, a static extension method is used to study the rheological processes of BMG Vit1, and associated with the results of differential scanning calorimetry (DSC) measurements. The correlation between structure transformation and property is also discussed.

2 EXPERIMENTAL

The glassy bulk metallic ingots, with composition of $Zr_{41}Ti_{14}Cu_{12.5}Ni_{10}Be_{22.5}$, were prepared by melting a mixture of elements of purity range from 99.5% to 99.9% under a titanium-gettered argon at-

① **Foundation item:** Projects(59971020; 50171028) supported by the National Natural Science Foundation of China; project(G-YW67) supported by Foundation of the Hong Kong Polytechnic University; project supported by Foundation of the State Key Lab of the Materials of Wuhan University of Technology, China
Received date: 2003 - 07 - 30; **Accepted date:** 2003 - 11 - 02
Correspondence: XIAO Jian-zhong, Professor; Tel: + 86-27-87544650; E-mail: jzxiao@public.wh.hb.cn

mosphere, then amorphous rods with the diameter of 14 mm were prepared by water quenching in silica tube. The amorphous nature of the as-quenched rods was ascertained with XRD. The experimental samples with sizes of 10 mm × 1 mm × 0.5 mm were cut from the amorphous rods. In order to eliminate the structure difference, the experimental samples were firstly heated above the glass transition temperature 633 K for 10 min. The amorphous nature of the pre-annealing sample was approved with the XRD again.

The static extension measurement of amorphous sample was carried out on a Perkin Elmer Pyris DMA7e dynamic thermal mechanical analyzer (DMA) under flowing argon atmosphere. The sample was loaded under room temperature, and then heated at the rate of 2.5, 5, 10 and 15 K/min, respectively. The relation between the sample length and temperature was recorded synchronously. In order to study the stress effect on strain and strain rate, the applied loads on the samples were 200, 800, 1 600 and 3 200 mN, respectively. The length accuracy of this experiment was ±50 nm. The furnace of the DMA was calibrated for temperature with high purity indium and zinc with an accuracy of ±(1 - 2) K.

The differential scanning calorimetry (DSC) measurements were employed under purified argon atmosphere in the Perkin Elmer DSC 7 at the heating rate corresponding to the static extension measurement. The calorimeter was calibrated for temperature at various heating rates with high purity indium and zinc with an accuracy of ±0.1 K. The values of the end temperature of glass transition, $T_{g\text{-end}}$, the onset temperature for multistep crystallization peak, $T_{xi\text{-onset}}$, were determined from the DSC traces with an accuracy of ±1 K. The apparent activation energy E for the glass transition and the crystallization transition can be evaluated by Kissinger's equation:

$$\ln \frac{T^2}{\varphi} = \frac{E}{RT} + \text{const} \qquad (1)$$

where T stands for $T_{g\text{-end}}$ or $T_{xi\text{-onset}}$, φ is the scanning rate in DSC, R is the gas constant. The apparent activation energy E can be deduced from the slope in curve of $\ln(T^2/\varphi)$ vs $1/T$.

3 RESULTS AND DISCUSSION

3.1 Glass transition and crystallization processes

The temperature dependences of strain (ε) and strain rate ($d\varepsilon/dt$) for BMG Vit1 is shown in Fig. 1. In the curve, it can be seen that the bulk metallic glass undergoes the glass state, supercooled liquid state and crystallization states in temperature range from room temperature to 760 K. In different temperature range, the temperature dependences of strain and strain rate are different. In the temperature range from room temperature to the onset temperature of viscous flow, T_g^v, the strain and strain rate increase slowly with elevation of temperature. But the strain and strain rate increase rapidly with increasing temperature in the temperature range from the onset temperature T_g^v of viscous flow to 760 K. It is seen that some strain rate peaks, marked as p_1^v, p_{1-b}^v, p_2^v and p_3^v, respectively, appear on temperature—strain rate curves. The values of the peak temperature are T_{p1}^v = 669.9 K, T_{p1-b}^v = 692 K, T_{p2}^v = 715.5 K and T_{p3}^v = 739.1 K, respectively. In DSC curve at the same heating rate, the characteristic temperatures of multi-step crystallization are $T_{x1\text{-onset}}$ = 669.4 K, $T_{x1b\text{-onset}}$ = 690.2 K, $T_{x2\text{-onset}}$ = 715.4 K and $T_{x3\text{-onset}}$ = 740.5 K, respectively. Thus it can be shown that the strain rate peaks are associated with the processes of multistep crystallization of BMG Vit1.

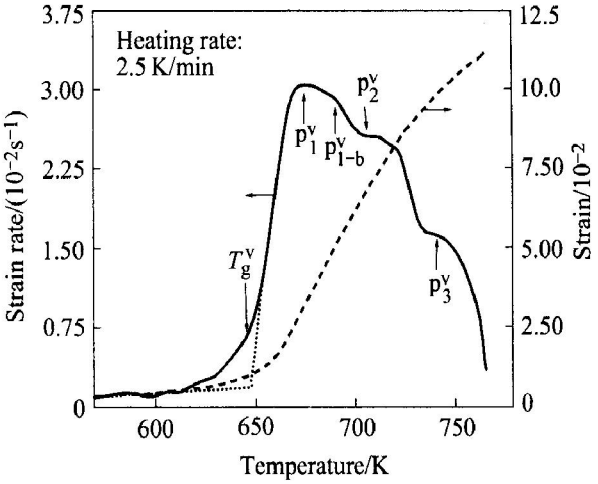

Fig. 1 Temperature dependence of strain and strain rate for BMG Vit1

The temperature dependence of the strain rate of the BMG Vit1 at various heating rates is shown in Fig. 2(a). The strain rate changes significantly at temperature T_g^v, and increases sharply with temperature increasing. But at temperature T_{p1}^v, the first strain rate peak p_1^v is formed, subsequently the strain rate starts to decrease. The DSC curves at heating rate corresponding to extension measurement are shown in Fig. 2(b). It can be seen from the above-mentioned two figures that the temperature dependence of the strain rate is well consistent with the corresponding DSC curves. Table 1 indicates the characteristic temperatures of glass transition and crystallization as well as the activation energy for BMG Vit1 obtained from the curves of DSC and strain rate. It shows that the onset temperature of viscous flow, T_g^v, the first and second strain rate peak temperatures, T_{p1}^v and T_{p2}^v, correspond respectively with the end temperature of glass transition $T_{g\text{-end}}$, the onset temperatures for the first and second crystallization peak, $T_{x1\text{-onset}}$ and $T_{x2\text{-onset}}$. Furthermore, the activation energies and their corresponding parts are approximately equal. Therefore it can be concluded that

the onset of viscous flow and the end of glass transition are interrelated, the first and second strain rate peaks correspond with the first and second crystallization transition processes, respectively. It is noticeable that at the heating rate of 2.5 K/min, the first exothermal crystallization peak in the DSC curves breaks into two peaks p_1 and $p_{1\text{-}b}$. The microcosmic transformation process also appears in the strain rate curves, namely, the corresponding maximums of the strain rate, p_1^v and $p_{1\text{-}b}^v$ occur.

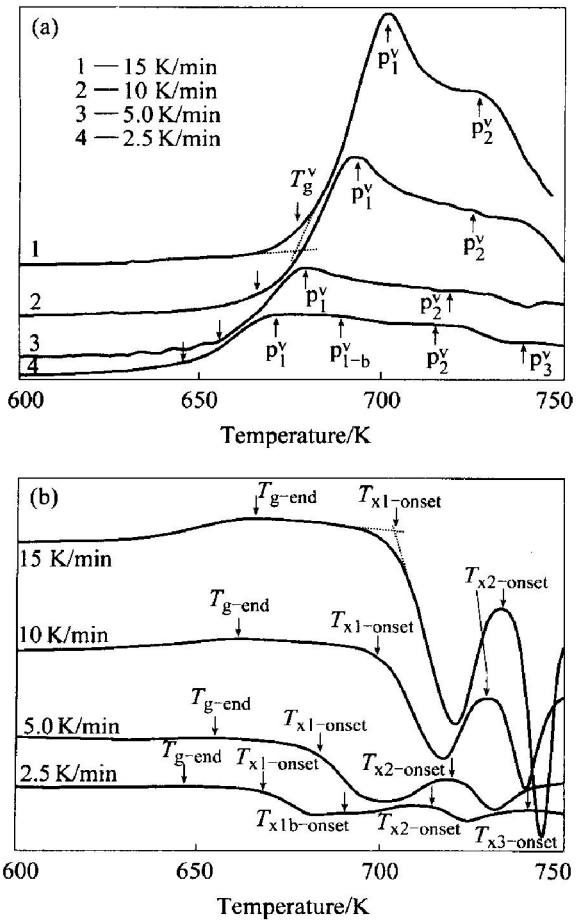

Fig. 2 Temperature dependences of strain rate curve (a) and DSC curves (b) for BMG Vit1 at various heating rates

Table 1 Characteristic temperature and activation energy of glass transition and crystallization for BMG Vit1 gained from curves of DSC and strain rate, respectively

Heating rate/(K·min^{-1})	DSC curve			Strain rate curve		
	$T_{g\text{-}end}$/K	$T_{x1\text{-}onset}$/K	$T_{x2\text{-}onset}$/K	T_g^v/K	T_{p1}^v/K	T_{p2}^v/K
2.5	644.1	669.4	715.4	645.2	669.9	715.5
5	654.5	681.8	720.5	654.4	680.2	719.2
10	665.4	693.6	729.5	666.5	692.4	728.9
15	670.0	700.6	733.0	671.6	702.3	731.5
E/(kJ·mol^{-1})	232.4	213.0	409.9	227.6	206.5	429.3

The observational results in both DSC and static extension measurement, in the final analysis, are due to the microstructure transformation of Vit1 BMG. Under continuous heating condition, one endothermal and three exothermal peaks appear in DSC curves (as shown in Fig. 2(b)). The endothermal peak is associated with glass transition process which is accompanied by structure transformation from solid state to supercooled liquid state. Three exothermal peaks are associated with multistep crystallization. The primary crystallization in Vit1 BMG results in the formation of spatially periodical arranges of Cu-Ti rich nanocrystals which is preceded by a modulated chemical decomposition process. Subsequently, at higher temperature, a Laves phase having the hcp $MgZn_2$-type structure appears[19]. The transformation process of microstructure also results in change of mechanical property such as strain rate in Fig. 2(a).

3.2 Rheological process

From Fig. 1 it can be inferred that the rheological characters of BMG Vit1 above and below the onset temperature of viscous flow are distinctly different. So the rheological behavior can be investigated in the two temperature range divided by T_g^v.

3.2.1 Elasticity and anelasticity below T_g^v

Fig. 3 shows the effect of stress on strain in temperature range below T_g^v. The relation between stress and strain in low temperature range is different from high temperature range. Below 573 K the stress dependence of the strain complies with the Hooke's law, namely, $\sigma = E\varepsilon$ (E is the elastic modulus). In Fig. 3 the stress dependences of the strain at 513 K, 533 K and 548 K are drawn as example. The results illuminate that the Vit1 exhibits elastic behavior below 573 K. However, as a result of anelasticity of the BMG Vit1, the stress dependences of the strain deflect from the linear relation above 573 K and the degree of departure increases with increasing temperature.

Below T_g^v, under static invariant stress condition, the overall strain of metallic glass can be expressed as[20]:

$$\varepsilon = \varepsilon_i + \varepsilon_a = \frac{\sigma}{G} + \frac{\sigma}{G_a}\left\{1 - \exp\left[-\left(\frac{t}{\tau}\right)^n\right]\right\} \quad (2)$$

where ε_i is the elastic strain, ε_a is the anelastic strain, G is the shear modulus of the material, G_a is the shear modulus of anelastic deformation, τ is the relaxation time of strain under invariant stress condition.

The relation between stress and strain in Fig. 3 can be well explained by Eqn. (2). At lower temperature, because of the low movement ability of atom, the relaxation time τ is so long that the second term in Eqn. (2) equals approximatively zero, namely, $\varepsilon \approx \sigma/G$, indicating that the rheological character ex-

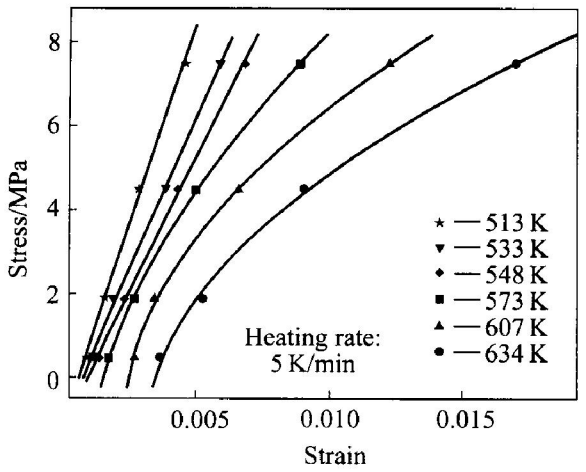

Fig. 3 Stress dependence of strain below onset temperature of viscous flow T_g^v

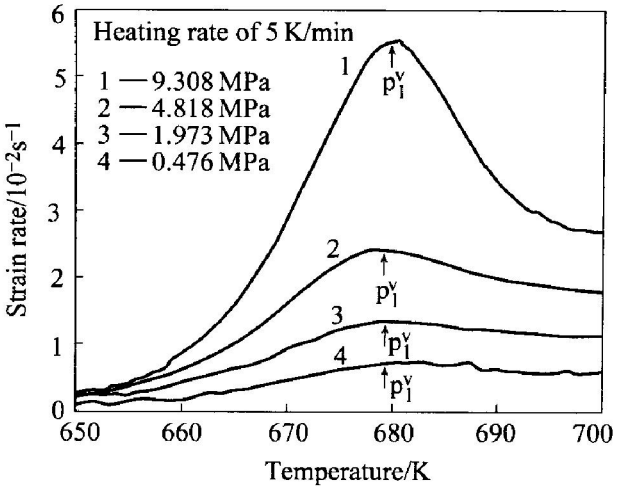

Fig. 4 Influence of stress on strain rate for BMG Vit1

hibits elasticity. In higher temperature range, the relaxation time τ is shortened significantly because the movement ability of atom is enhanced distinctly, so the contribution of the anelastic strain in metallic glasses to overall strain is too great to be neglected, i. e. the stress dependence of overall strain deflects from the linear relation. The higher the temperature is, the less the relaxation time τ, the more the anelastic strain, and the more the stress dependence of overall strain deflects from the linear relation.

3.2.2 Newtonian viscosity above T_g^v

In order to study the rheological character of BMG Vit1 above T_g^v, the temperature dependence of strain rate ($d\varepsilon/dt$) under various stress(σ) condition was measured (as shown in Fig. 4). For different stresses, the positions of the strain rate peaks seem not to change, and the higher the stress level, the higher the strain rate peak is. Moreover, it is seen from Fig. 5 that a linear relation exists between strain rate and stress. The results show that the stress dependence of strain rate accords with the Newtonian rheological law and can be expressed as:

$$\frac{d\varepsilon}{dt} = a + b\sigma \tag{3}$$

where a and b are fitting parameters. The first term, a, which is independent of the stress, is due to the contribution from the structure relaxation of supercooled liquid. We deduced from linear fitting the values of a and b, $-2.96\times10^{-9}\ s^{-1}$ and $6.33\times10^{-9}\ Pa^{-1}s^{-1}$, respectively. So the rheological behavior of BMG Vit1 exhibits the character of Newtonian viscous flow in supercooled liquid state. Nieh[18] reported similar result in other BMG $Zr_{10}Al_5Ti_{17.9}Cu_{14.6}Ni_{52.5}$ system.

Thus it can be seen that, with increase of temperature, the rheological processes change from elasticity to anelasticity, finally to the Newtonian viscous flow in BMG Vit1.

For Newtonian viscous flow, the stress (σ) dependence of strain rate ($d\varepsilon/dt$) can be expressed as:

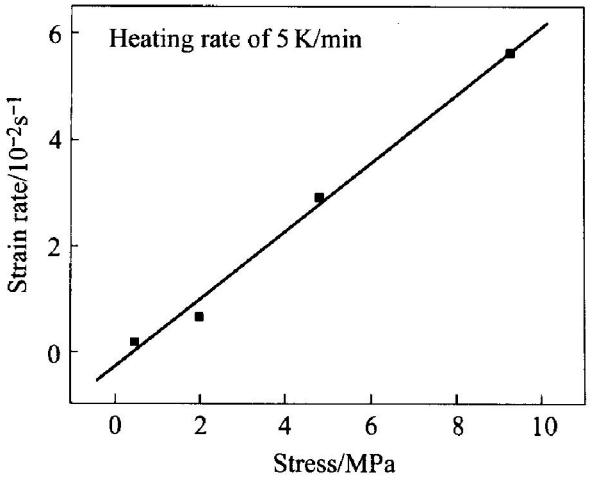

Fig. 5 Stress dependence of strain rate at peak temperature (680 K)

$$\frac{d\varepsilon}{dt} = \frac{\sigma}{3\eta} \tag{4}$$

where η is viscosity. From Eqn. (4) it is known that the maximum of strain rate corresponds with the minimum of viscosity.

According to the classical theory, the crystal nucleation rate per unit volume, I_v, and the growth of the nuclei, u, are described by[21]

$$I_v = \frac{A_v}{\eta}\exp\left[-\frac{16\pi\sigma^3}{3k_BT(\Delta g)^2}\right] \tag{5}$$

$$u = \frac{k_BT}{3\pi l^2\eta}\left[1-\exp\left(-\frac{V\Delta g}{k_BT}\right)\right] \tag{6}$$

where A_v is a constant of the order of 10^{32} Pa·s/(m^3·s) for homogeneous nucleation, η is the viscosity, Δg is the difference in Gibbs free energy (per unit volume), k_B is Boltzmann constant, σ is the interfacial energy between the liquid and the nuclei, l is the average atomic diameter and V is the atom volume.

Generally, the start of crystallization process takes place at the easiest position for nucleation and

the growth of the nuclei, i. e. I_v and u reach maximum. By Eqns. (5) and (6), the maximum values of I_v and u correspond with the minimum of viscosity, namely, the maximum of strain rate. Thereby the strain rate reaches the maximum at the onset temperature for multistep crystallization peak.

4 CONCLUSION

The temperature dependence of strain and strain rate of BMG Vit1 under constant heating condition was derived from the static extension method with DMA. A few strain rate peaks, which correspond to the glass transition and multistep crystallization in the DSC curves, were observed in relative curves between strain rate and temperature. The onset of viscous flow and the end of glass transition are interrelated, and the first and second strain rate peaks correspond with the first and second crystallization transition processes, respectively. By studying the effect of stress on strain and strain rate, it is found that the rheological behaviour of BMG Vit1 changes from elasticity to anelasticity, finally to the Newtonian viscous flow along with increasing of temperature.

Acknowledgements

The authors wish to thank Prof. W. H. Wang for furnishing BMG samples to us.

REFERENCES

[1] Klement W, Willens R, Duwez P. Non-crystalline structure in solidified gold-silicon alloys[J]. Nature, 1960, 187(4740): 869-870.

[2] Inoue A, Zhang T, Masurmoto T. Al-La-Ni amorphous alloys with a wide supercooled liquid region[J]. Mater Trans JIM, 1989, 30: 965-972.

[3] Inoue A, Nishiyama N, Matsuda T. Preparation of bulk glassy $Pd_{40}Ni_{10}Cu_{30}P_{20}$ alloy of 40 mm in diameter by water quenching[J]. Mater Trans JIM, 1996, 37(2): 181-184.

[4] Inoue A, Zhang T. Fabrication of bulk glassy $Zr_{55}Al_{10}Ni_5Cu_{30}$ alloy of 30 mm in diameter by a suction casting method[J]. Mater Trans JIM, 1996, 37(2): 185-187.

[5] Peker A, Johnson W L. A highly processable metallic glass: $Zr_{46.75}Ti_{8.25}Cu_{7.5}Ni_{10}Be_{27.5}$[J]. Appl Phys Lett, 1993, 63(17): 2342-2344.

[6] Kim Y J, Busch R, Johnson W L, et al. Metallic glass formation in highly undercooled $Zr_{41.2}Ti_{13.8}Cu_{12.5}Ni_{10.0}Be_{22.5}$ during containerless electrostatic levitation processing[J]. Appl Phys Lett, 1994, 65(17), 2136-2138.

[7] Waniuck T A, Busch R, Masuhr A, et al. Equilibrium viscosity of the $Zr_{41}Ti_{14}Cu_{12.5}Ni_{10}Be_{22.5}$ bulk metallic glass-forming liquid and viscous flow during relaxation, phase separation, and primary crystallization[J]. Acta Mater, 1998, 46(15): 5229-5236.

[8] Hays C C, Kim C P, Johnson W L. Large supercooled liquid region and phase separation in the Zr-Ti-Ni-Cu-Be bulk metallic glasses[J]. Appl Phys Lett, 1999, 75(8): 1089-1091.

[9] PAN Ming-xiang, WANG Jing-guo, YAO Yu-shu, et al. Phase transition of $Zr_{41}Ti_{14}Cu_{12.5}Ni_{10}Be_{22.5}$ bulk amorphous below glass transition temperature under high pressure[J]. Appl Phys Lett, 2001, 78(5): 601-603.

[10] WANG W H, WU E, WANG R J, et al. Phase transformation in a $Zr_{41}Ti_{14}Cu_{12.5}Ni_{10}Be_{22.5}$ bulk amorphous alloy upon crystallization[J]. Phys Rev B, 2002, 66(10): 104205-1-104205-5.

[11] Löffler J F, Johnson W L. Model for decomposition and nanocrystallization of deeply undercooled $Zr_{41.2}Ti_{13.8}Cu_{12.5}Ni_{10.0}Be_{22.5}$[J]. Appl Phys Lett, 2000, 76(23): 3394-3396.

[12] Lu J, Ravichandran G, Johnson W L. Deformation behavior of the $Zr_{41.2}Ti_{13.8}Cu_{12.5}Ni_{10}Be_{22.5}$ bulk metallic glass over a wide range of strain-rates and temperatures [J]. Acta Materialia, 2003, 51(12): 3429-3443.

[13] Bruck H A, Christman T, Rosakis A J, et al. Quasi-static constitutive behavior of $Zr_{41.25}Ti_{13.75}Ni_{10}Cu_{12.5}Be_{22.5}$ bulk amorphous alloys[J]. Scripta Metall, 1994, 30(4): 429-434.

[14] Busch R, Kim Y J, Johnson W L. Thermodynamics and kinetics of the undercooled liquid and the glass transition of the $Zr_{41.2}Ti_{13.8}Cu_{12.5}Ni_{10.0}Be_{22.5}$ alloy[J]. J Appl Phys, 1995, 77(8): 4039-4043.

[15] Geyer U, Schneider S, Johnson W L, et al. Atomic diffusion in the supercooled liquid and glassy states of the $Zr_{41.2}Ti_{13.8}Cu_{12.5}Ni_{10}Be_{22.5}$ alloy[J]. Phys Rev Lett, 1995, 75(12): 2364-2367.

[16] ZHANG Ke-qin, CHEN Yan, GUAN Ying, et al. Crystallization kinetics of $Zr_{41}Ti_{14}Cu_{12.5}Ni_{10}Be_{22.5}$ bulk metallic glass[J]. Trans Nonferrous Met Soc China, 2002, 12(2): 280-282.

[17] Lee K S, Ha T K, Ahn S, et al. High temperature deformation behavior of the $Zr_{41.2}Ti_{13.8}Cu_{12.5}Ni_{10}$-$Be_{22.5}$ bulk metallic glass [J]. Journal of Non-Crystalline Solids, 2003, 317(1-2): 193-199.

[18] Nieh T G. Deformation of metallic glasses with special emphasis in supercooled liquid region[J]. Trans Nonferrous Met Soc China, 2002, 12(4): 726-733.

[19] Schneider S, Thiyagarajan P, Johnson W L. Formation of nanocrystals based on decomposition in the amorphous $Zr_{41.2}Ti_{13.8}Cu_{12.5}Ni_{10}Be_{22.5}$ alloy[J]. Appl Phys Lett, 1996, 68(4): 493-495.

[20] Luborsky L E. Amorphous Metallic Alloys[M]. London: Butterworths, 1983.

[21] Inoue Akihisa. Bulk Amorphous Alloys: Preparation and Fundamental Characteristics [M]. Switzerland: Trans Tech Publications Ltd, 1998.

(Edited by YUAN Sai-qian)